Deep Resources Engineering 3 (2026) 100250

Contents lists available at ScienceDirect

Deep Resources Engineering

journal homepage: www.keaipublishing.com/en/journals/deepre/

Full length article

A machine learning based attitude control model for open-type TBMs on the spiral ramp of Beishan underground research laboratory

Qixin Xu [a], Qiuming Gong [a,*], Liu Huang [a], Ju Wang [b,c], Hongsu Ma [b,c], Mengxue Qi [d], Bei Han [a]

[a] Key Laboratory of Urban Security and Disaster Engineering of Ministry of Education, Beijing University of Technology, Beijing 100124, China
[b] Division of Environmental Engineering, Beijing Research Institute of Uranium Geology, Beijing 100029, China
[c] CAEA Innovation Center for Geological Disposal of High-Level Radioactive Waste, Beijing 100029, China
[d] TBM Technology Research Institute, China Railway 18th Bureau Group Tunnel Engineering Co., Ltd., Chongqing 400700, China

ARTICLE INFO

Keywords:
Open-type TBM
Spiral ramp
Attitude control
Machine learning method

ABSTRACT

Precise attitude control of Tunnel Boring Machines (TBM) is critically important for ensuring tunneling quality and safety, especially in tunnels with steep slopes, long curves, or small turning radii. However, the tunneling trajectory is susceptible to deviations from the designed tunnel axis (DTA) due to the effect of a variety of factors including rock mass conditions, TBM tunneling parameters, operator's expertise, and the designed tunnel axis complexities. This study addresses this vital need through a machine learning based approach for attitude adjustment. The theoretical analysis of the steering mechanism of the open-type TBM shows the horizontal attitude control is primarily governed by the stroke difference of lateral gripper cylinders, while vertical control is governed by the mean stroke of the torque cylinders. Depending on the spiral ramp in the Beishan Underground Research Laboratory project in Gansu Province, China, TBM tunneling data and guidance data were collected. Through a series of preprocessing steps, four key feature categories were fused, and a comprehensive attitude database was set up. Three machine learning models were developed for the real-time attitude adjustment. Among three models, the LightGBM algorithm delivered the best performance, achieving a mean absolute error (MAE) of 1.764 mm and root mean square error (RMSE) of 2.082 mm in horizontal control, and an MAE of 1.370 mm with RMSE of 1.564 mm in vertical control. The model validation using data from other sections of the spiral ramp, including both straight and curved sections, demonstrated that the performance was consistent with test results. It confirmed the model's robustness and applicability in practical engineering condition.

1. Introduction

With the research and development of the high-level waste disposal in China entering the underground laboratory stage [1], TBM tunnelling method has been applied to excavate the spiral ramp due to its advantages of fast excavation speed, small construction impact area, and relatively favorable construction environment, which corresponds to the requirements of controllable and minimized damage zones of tunnel systems in the underground laboratory. Due to the uncertainty of the surrounding rock mass conditions, the TBM specifications and the operator's expertise and other factors, it is difficult to control the attitude during the TBM tunnelling. Especially in the tunnel with steep gradients and long curved section, the precise control of the tunnel boring machine's attitude is crucial. However, due to the complexity of the geological conditions and the influence of these TBM tunnelling parameters, the TBM will inevitably generate an attitude deviation during the tunneling process. It requires the continuous dynamic attitude adjustment.

The TBM's guidance system monitors the TBM's attitude and dynamically transmits corrective orders to ensure that the axis of the constructed tunnel coincides with the axis of the designed tunnel. In the research on the attitude control of tunnel boring machine, many studies have been related to the attitude control of the shield machine. Shield machine attitude is typically controlled by regulating hydraulic cylinders, often using methods like Proportional Integral Derivative (PID) or fuzzy logic. Manabe et al. [2] developed an automatic control system by modeling the relationship between the head inclination and machine attitude deviation by using a PID controller to dynamically adjust

Peer review under responsibility of Editorial Board of of Deep Resources Engineering.

* Corresponding author.
E-mail address: gongqiuming@bjut.edu.cn (Q. Gong).

https://doi.org/10.1016/j.deepre.2026.100250
Received 27 October 2025; Received in revised form 24 January 2026; Accepted 23 February 2026
Available online 26 February 2026

hydraulic cylinder pressure. Zhou et al. [3] combined fuzzy logic with PID control to achieve quantitative output of attitude control parameters. Gong et al. [4] established a dual closed-loop feedback mechanism, creating a mathematical relationship between the shield attitude and differential speeds of left/right thrust cylinders, and implemented a fuzzy PID strategy for cylinder velocity regulation. To reduce complexity, Li et al. [5] simplified the complex fuzzy control architecture from multiple inputs by designing a two-dimensional controller that processes horizontal and vertical deviations simultaneously. Furthermore, Zhang et al. [6] addressed multi-cylinder coordination by developing a cascade control system based on multi-constraint fuzzy rules.

Although fuzzy logic and PID control are capable of real-time control, these methods have limitations. Fuzzy control relies on predefined expert rules, which are difficult to establish for complex geological conditions and varying tunnel alignments. PID control, with its simple processing of input data, often lacks the precision required for such a complex system. To overcome these challenges, researchers have explored model-based approaches. Yang et al. [7] proposed a synchronous control strategy for multiple thrust cylinders based on displacement control in the propulsion system of shield tunneling machines. Wang et al. [8] designed a multi-cylinder control model that achieved attitude adjustment by varying the lengths of its kinematic chains. Other studies have focused on the optimization and simulation under specific conditions. Liu et al. [9] achieved efficient deviation control in compound formations by optimizing the thrust and propulsion speed of the shield machine, while Xie et al. [10] developed a condition-adapted attitude control model through hydraulic system analysis and simulation tests. Yue et al. [11] established a double-closed-loop control model by utilizing the shield's kinetic equations to regulate its attitude through cylinder parameters.

Additionally, data-driven and geology-integrated methods have been developed. Hu et al. [12] proposed a big data-driven system that calculates cylinder pressures in real-time based on target positions. Zhu et al. [13] integrated geological data to automatically adjust the shield's steering mechanism, ensuring it followed the designed tunnel axis. Ultimately, all the mentioned methods achieved shield machine attitude control by regulating hydraulic cylinder parameters.

The attitude control mechanism for hard rock TBM is different from that of the shield machine due to different geological conditions and load-bearing characteristics, therefore the attitude control strategies cannot be directly transferred. Researchers have developed methods specific to hard rock TBMs. Zhang et al. [14] established attitude control formulae for various tunnel curves and proposed a synchronous control method for bilateral gripper cylinders. Zhang et al. [15] established a mechano-hydraulic coupling model of the regripping cycle that accounted for rock mass characteristics to achieve the TBM's attitude control. Peng et al. [16] identified a linear relationship between the pitch angle and torque cylinders within a small angular range that effectively reduced displacement control deviation. Liu et al. [17] designed a dynamic mathematical model for hard rock TBM and designed a control scheme to achieve horizontal and vertical attitude control. Zhang [18] realized automated vertical control by analyzing the force mechanism of the gripper and modeling the hydraulic system, correlating the pressure distribution with surrounding rock mass forces. For multi-cylinder systems, Liu [19] proposed a coordinated control method based on surrounding rock mass load-characteristic and mechanical configuration topology. Additionally, coordinated multi-system control strategies have been established [20,21]. These approaches are supported by electro-mechanical-hydraulic coupling dynamics models based on the Lagrangian method and ACR nonlinear processing techniques to enable precise control in complex geological conditions.

Current research on TBM attitude control faces several limitations. The available datasets are often restricted to a single type, rarely integrating both tunneling and guidance data. This lack of multi-source data hinders the accurate modeling of coupled parameter interactions and their relationship with attitude changes. Furthermore, few studies analyze the impact of the mechanical steering structure on the attitude deviation of the open-type TBM. The precision of existing methods is often compromised due to inadequate processing of raw tunneling and guidance data. To address these gaps, this study used data from the spiral ramp project at the Beishan Underground Research Laboratory. We first collected and processed both tunneling and guidance data, then conducted a theoretical analysis of the open-type TBM's steering mechanism. Finally, we constructed an intelligent attitude control model using machine learning algorithms to provide a more robust and adaptive attitude control instruction to support the spiral ramp construction.

2. Project overview

2.1. The spiral ramp

This study was conducted on the Beishan Underground Laboratory project, China's first underground research facility dedicated to the geological disposal of high-level radioactive waste. The Beishan Underground Research Laboratory is internationally recognized as a "third-generation underground laboratory" [1]. It represents a pivotal scientific platform for advancing China's geological disposal technologies for high-level radioactive waste. The facility lies within the Xinchang candidate site of the Beishan preselected area, hosted within an intact granitic rock mass in the Gobi Desert [22]. The underground facility consists of a spiral ramp with a progressively increasing inclination, three vertical shafts (one personnel shaft and two ventilation shafts), and two horizontal research tunnels.

Based on comprehensive feasibility analyses, the TBM method was employed for the construction of the spiral ramp [23]. The ramp included the key design parameters of a total length of 7.5 km, an excavation diameter of 7.03 m, a maximum overburden depth of 560 m, an average longitudinal gradient of 9% (with a maximum of 10%), and a curvature radius of 380 m.

This configuration produces a three-dimensional spiral structure reaching a vertical depth of 560 m, as shown in Fig. 1. The spiral configuration causes continuous changes in tunnel alignment both horizontally and vertically, requiring operators to make real-time adjustments to the TBM to maintain the required curvature and gradient during tunneling. In addition, the combination of continuous downward tunneling and curved advance exposes the cutterhead and steering systems to uneven dynamic loads. These conditions increase project risks by leading to gradual deviations in machine attitude over time, which significantly complicate the control of the TBM's attitude and may require costly rework, as well as accelerated cutter wear due to the uneven loads.

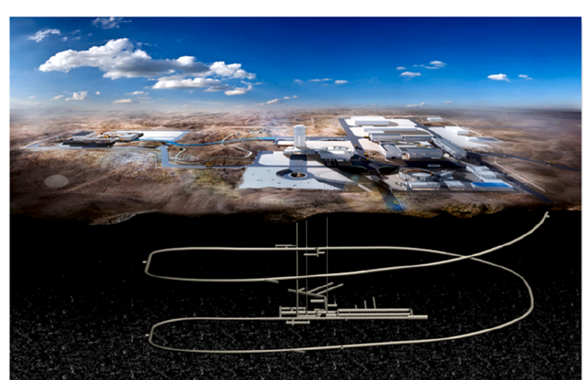

Fig. 1. Schematic diagram of the spiral ramp of Beishan Underground Laboratory [1].

The TBM method was employed to excavate the spiral ramp extending from mileage K0 + 494.700 to K7 + 507.507, with a total of 7 curved sections and 8 straight sections. All curved sections maintain identical design parameters, and its horizontal turning radius is 255 m. The schematic diagram of the main structure of the ramp is shown in Fig. 2.

2.2. Rock mass conditions along the spiral ramp

The spiral ramp is excavated in granitic rock masses that exhibit high integrity, as indicated by a Rock Mass Rating (RMR) of over 85. It contains discontinuous veins of tonalite and pegmatite, typically less than 2 m in thickness, including minor granite and diorite. The mechanical properties show notable variability, with a saturated uniaxial compressive strength ranging from 105 to 249 MPa and averaging 161 MPa, indicating a transition between extremely hard and hard rock.

The host rock mass has very low permeability, measured at 3.2×10^{-7} cm/s. Groundwater recharge is minimal and negligible, occurring primarily through limited rainfall infiltration. The groundwater is weakly corrosive, presenting no significant risk to the engineering construction.

2.3. TBM specifications

"Beishan NO.1" open-type TBM (Fig. 3) was used to excavate the spiral ramp, which was developed by Beijing Geological Research Institute of Nuclear Industry of CNNC, China Railway Construction Heavy Industry Group Corporation (TBM manufacturer) and China Railway 18th Bureau Group Corporation [24]. The design specifications of the open-type TBM were detailed in Table 1.

3. Steering mechanism of the open-type TBM

"Beishan NO.1" TBM utilizes a main beam steering system, where horizontal attitude steering is achieved through lateral gripper cylinders while vertical steering is achieved through torque cylinders [25].

3.1. Horizontal steering

The schematic diagram of the horizontal steering is shown in Fig. 4. The extension/retraction of the lateral gripper cylinders induces the horizontal displacement of the main beam, where Δx_1 represents half of the difference between the left and right gripper cylinders strokes. The thrust cylinders propel the machine forward by a distance of s, while α signifies the horizontal swing angle. R denotes the horizontal turning radius, and L_1 refers to the distance from the midpoint of the lateral cylinder to the midpoint of the cutterhead.

The midpoint of the cutterhead passes through the axis of the excavation tunnel and the main beam is always tangent to the excavation trajectory, which leads to:

$$[(L_1+s)\sin\alpha-\Delta x_1-R]^2+[(L_1+s)\cos\alpha-L_1]^2=R^2 \tag{1}$$

$$\frac{(L_1+s)\cos\alpha-L_1}{(L_1+s)\sin\alpha-\Delta x_1-R}\cdot\frac{(L_1+s)\cos\alpha}{(L_1+s)\sin\alpha}=-1 \tag{2}$$

By integrating Eq. (1) and Eq. (2), we derive:

$$\Delta x_1{}^2+2\Delta x_1R-2L_1s-s^2=0 \tag{3}$$

The connection between the distance s and the horizontal angle α is established:

$$s=R\tan\alpha+\frac{L_1}{\cos\alpha}-L_1 \tag{4}$$

By combining Eq. (3) and Eq. (4), we can eliminate the influence of the distance s:

$$\Delta x_1{}^2+2R\Delta x_1-2L\left(R\tan\alpha+\frac{L_1}{\cos\alpha}-L_1\right)-\left(R\tan\alpha+\frac{L_1}{\cos\alpha}-L_1\right)^2=0 \tag{5}$$

Therefore the horizontal swing angle α can be expressed as:

$$\alpha=\frac{\pi}{2}-\left[\arctan\left(\frac{L_1}{R+\Delta x_1}\right)+\arcsin\left(\frac{R}{\sqrt{(R+\Delta x_1)^2+L_1{}^2}}\right)\right] \tag{6}$$

The relationship between the horizontal deviation Δh of the cutterhead and the swing angle α is as follows:

$$\Delta h=R(1-\cos\alpha) \tag{7}$$

Substituting Eq. (6) into Eq. (7) finally yields the theoretical relationship linking the horizontal deviation Δh of the cutterhead and half of

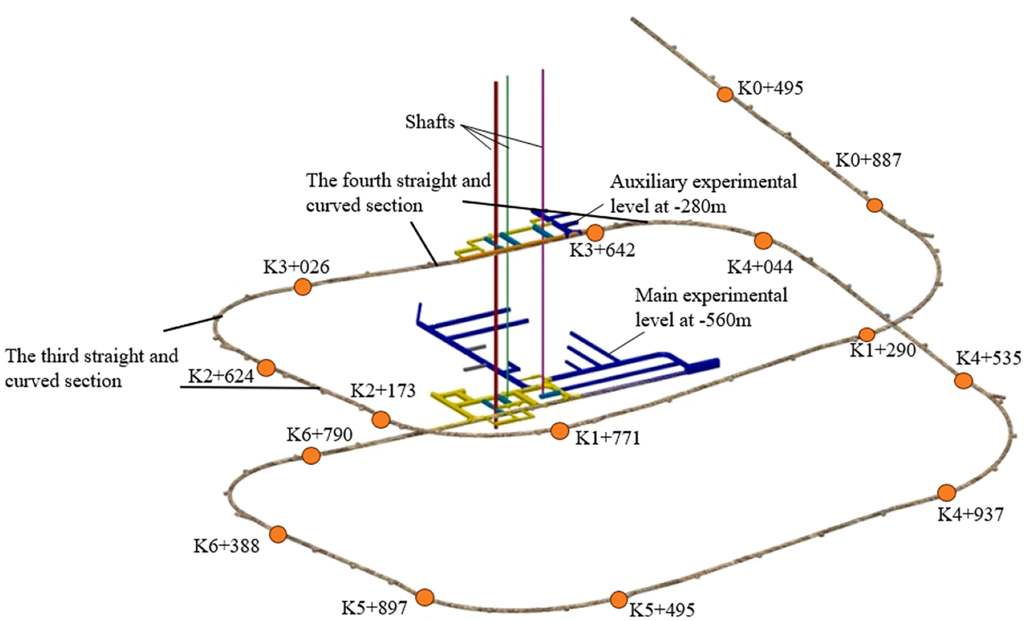

Fig. 2. Schematic diagram of the main structure of the spiral ramp project.

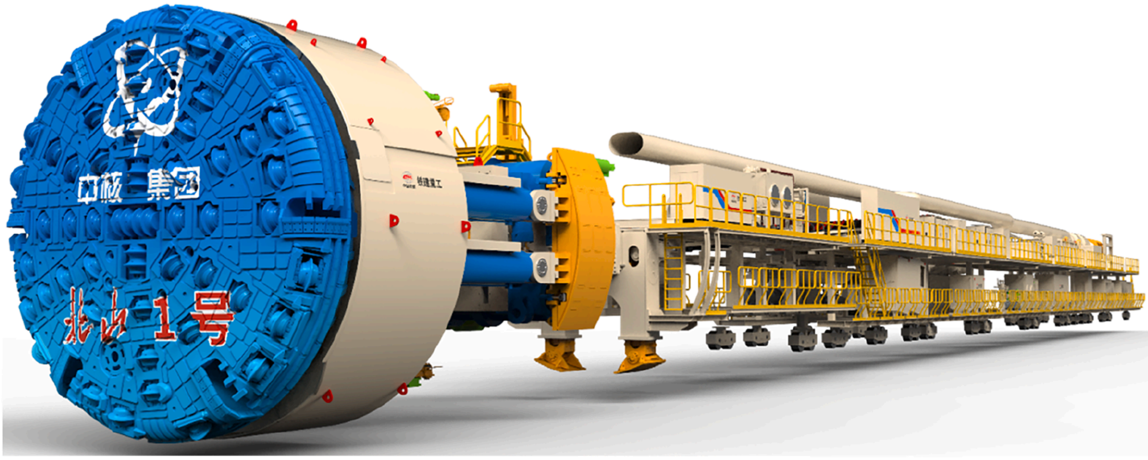

Fig. 3. The open-type TBM “Beishan NO.1”.

Table 1
Technical parameters of TBM.

Technical parameters	Design value
Cutterhead diameter	7030 mm
Cutterhead power	6×400 kW
Rated torque	5160 kN·m
Cutterhead rotating speed	0–10 r/min
Maximum thrust	23,562 kN
Disc cutters type	Center Cutters: 18" (457 mm) Face & Gauge Cutters: 20" (508 mm)
Disc cutter configuration	4×center cutters, 35×single disc face cutters, 12×gauge cutters
Thrust cylinder stroke	1850 mm

the difference between the left and right gripper cylinders Δx_1:

$$\Delta h = R\left[1 - \frac{\sqrt{\Delta x_1{}^2 + 2R\Delta x_1 + L_1{}^2}\left(R + \Delta x_1\right) - RL_1}{\left(R + \Delta x_1\right)^2 + L_1{}^2}\right] \tag{8}$$

3.2. Vertical steering

The schematic diagram of the vertical steering is shown in Fig. 5. The adjustment of the torque cylinders generates a vertical main beam displacement, where the mean stroke of the left and right torque cylinders is Δx_2. It makes the change of the TBM pitch angle β. The radius of the cutterhead is denoted as r, the length between the torque cylinders and the midpoint of the cutterhead as L_2.

The geometric relationship between the pitch angle β and the mean stroke of the left and right torque cylinders Δx_2 is expressed as:

$$\frac{r}{\sin\beta} + L_2 = \frac{r + \Delta x_2}{\tan\beta} \tag{9}$$

Isolating β from Eq. (9) yields:

$$\beta = \arcsin\left(\frac{-2rL_2 + \sqrt{4r^2L_2{}^2 + 4\left[L_2{}^2 + (r + \Delta x_2)^2\right]\left(\Delta x_2{}^2 + 2r\Delta x_2\right)}}{2\left[L_2{}^2 + (r + \Delta x_2)^2\right]}\right) \tag{10}$$

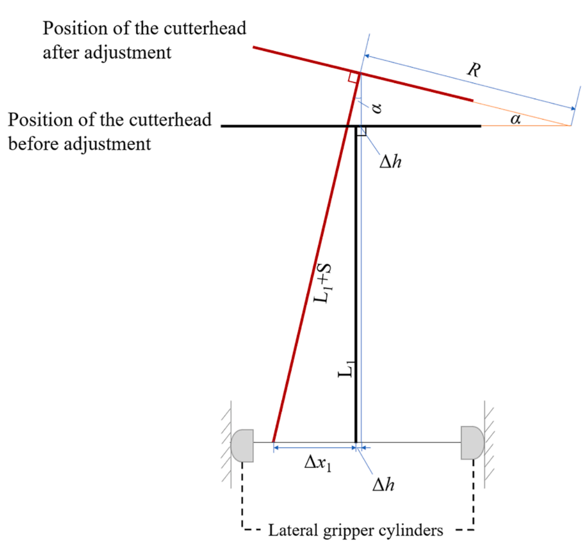

Fig. 4. Horizontal steering schematic diagram of the TBM.

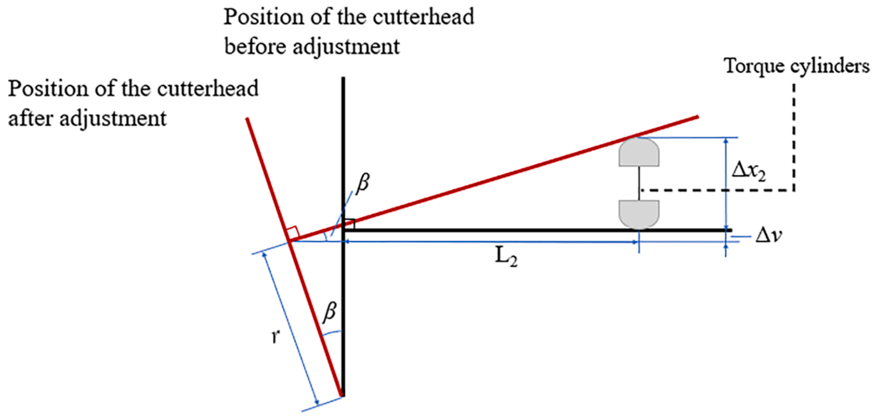

Fig. 5. Vertical steering schematic diagram of the TBM.

The relationship between the vertical deviation Δv of the cutterhead and the pitch angle β is as follows:

$$\Delta v = r(1 - \cos\beta) \tag{11}$$

Substituting Eq. (10) into Eq. (11) yields the theoretical relationship linking the vertical deviation Δh of the cutterhead and the mean stroke of the left and right torque cylinders Δx_2:

$$\Delta v = r\left[1 - \frac{\sqrt{[{L_2}^2 + (r+\Delta x_2)^2](r^2 + {L_2}^2) + 2rL\{\sqrt{r^2{L_2}^2 + [{L_2}^2 + (r+\Delta x_2)^2](\Delta {x_2}^2 + 2r\Delta x_2)} - 1\}}}{{L_2}^2 + (r+\Delta x_2)^2}\right] \tag{12}$$

As indicated by Eq. (8) and Eq. (12), the determined factors of the attitude deviation of the open-type TBM include not only the geometry specifications of the TBM, the design parameters of the spiral ramp, but also the extension/retraction of the lateral gripper cylinders and torque cylinders. But, the attitude control of the TBM can essentially be achieved by adjusting two types of cylinders.

The theoretical derivation establishes the existing physical relationship between cylinder strokes and cutterhead deviation. However, the derivation represents an idealized scenario, during actual construction process, factors such as varying rock mass conditions, dynamic rock-breaking vibrations and the non-rigid nature of mechanical structures also cause the actual attitude deviation that is different from the theoretical equations. To address these, this study employs a machine learning model trained on extensive operational data to uncover the coupled relationships among various factors. The model takes the current attitude deviation as input and provides recommended adjustments for the control cylinders to the operator, thereby facilitating real-time correction.

4. Attitude control modeling

4.1. Problem analysis

During the tunneling process from the moment of which the cutterhead contacts with the excavation face until the tunneling ceases, onboard sensors systematically record tunneling data and guidance data. Based on the real-time feedback from the guidance interface and operational experience, the TBM operator adjusts the attitude control cylinders. These adjustments significantly influence the TBM's attitude variation, which is also affected by the attitude control mechanism, surrounding rock mass conditions, design tunnel alignment and advance attitude status.

These monitored parameters can be categorized into three groups: tunneling parameters, attitude control parameters, and attitude parameters. The tunneling parameters reflect the rock–machine interaction and rock mass conditions during excavation, such as cutterhead thrust and torque, which are passive feedback data. Deep learning techniques may be used to identify the rock mass condition from sequences of tunneling parameters [26]. The attitude control parameters are set by the operator to regulate the TBM's attitude such as the strokes

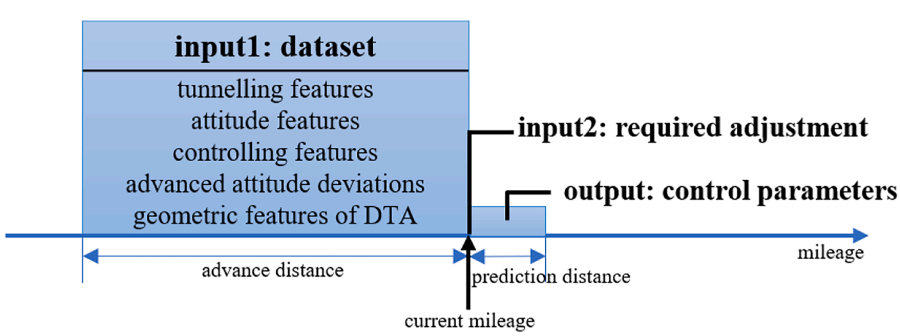

Fig. 6. Schematic of the attitude control model workflow.

of the gripper cylinders. The attitude parameters describe the real-time attitude deviations of the TBM, including the horizontal and vertical deviations of the cutterhead.

The proposed attitude control model should establish a mapping relationship among TBM tunneling parameters, attitude parameters, required input correction deviations, the geometric features of the designed tunnel alignment and the expected output attitude control parameters. The functional representation of the model is given as:

$$G_1 = g(\Delta_1, \Delta_2, \{P_{ij}\}, A, DTA) \tag{13}$$

where G_1 denotes the attitude control parameters output by the model; $g(\bullet)$ represents the trained mapping function of the control model; Δ_1 refers to the sequence of advance attitude deviations; Δ_2 indicates the required attitude adjustment; P_{ij} corresponds to the feature representation of the j-th tunneling features of the i-th tunneling feature sequence; A represents other relevant attitude features; and DTA describes the geometric characteristics of the designed tunnel axis.

For dataset temporal processing, sequences of attitude deviation vectors, tunneling features, and other relevant attitude features are used as input datasets to predict attitude control parameters, as illustrated in Fig. 6. This sequential design ensures the model captures dynamic temporal dependencies throughout the tunneling process.

4.2. Machine learning framework

To address the challenges of precise TBM steering in the spiral ramp, this study focuses on the complex, nonlinear interactions among multi-source parameters. Three advanced machine learning models: LightGBM, Random Forest, and XGBoost were employed to develop the robust TBM attitude control model. LightGBM is a high-performance gradient boosting framework that uses tree-based learning and employs leaf-wise growth strategy to achieve high efficiency and accuracy, particularly suitable for large-scale and high-dimensional data. Random Forest is an ensemble learning method that constructs multiple decision trees during training and combines their outputs to improve generalization and control over-fitting. XGBoost is another scalable gradient tree boosting model to optimize distribution and computation efficiency through parallel processing and regularization.

The framework is designed for a comparative analysis. Each candidate model was trained and evaluated on the same pre-processed data under a unified experimental setup. This systematic comparison serves to identify the most promising model for the TBM attitude control task.

4.3. Feature selection

The TBM's PLC and VMT systems record extensive operational parameters and attitude control parameters. However, most parameters (e.g., motor currents, coolant temperatures, and gas concentrations) have negligible influence on attitude adjustment. Initial feature selection therefore retains only those parameters directly involved in attitude control, such as strokes of the left/right gripper cylinders, left/right

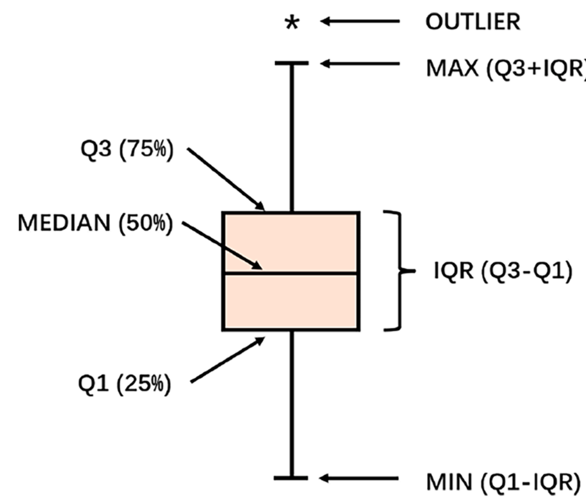

Fig. 7. Box-and-whisker plot.

torque cylinders, and shield cylinders. Furthermore, feature engineering is applied to generate three derived parameters through computational analysis:

(1) Half the difference between the lateral gripper cylinders strokes (ΔG): $\frac{G_{\text{left}} - G_{\text{right}}}{2}$

(2) Mean torque cylinder strokes ($\overline{T}$): $\frac{T_{\text{left}} + T_{\text{right}}}{2}$

(3) Increment of the horizontal deviation (ΔH): $H_t - H_{t-1}$

The selected features set retains critical indicators: cutterhead thrust, cutterhead torque, and penetration rate. This systematic selection process reduces dimensionality while preserving kinematic relationships essential for attitude control modeling.

Some features retained from the initial filtering exhibit a high degree of mutual correlation. To mitigate the negative impact of redundant features on the performance of the attitude control model, we further applied feature selection based on Pearson's correlation coefficient, defined as:

$$R = \frac{\sum_{i=1}^{n}(X_i - \overline{X})(Y_i - \overline{Y})}{\sqrt{\sum_{i=1}^{n}(X_i - \overline{X})^2}\sqrt{\sum_{i=1}^{n}(Y_i - \overline{Y})^2}} \tag{14}$$

The value of R represents the correlation degree between two features. A positive R indicates a positive correlation, while a negative R indicates a negative correlation. The closer to 1 or –1 the R, the stronger the correlation is. In this study, a correlation threshold of 0.8 was adopted. For any feature pair with $|R| > 0.8$, only one feature was retained to enhance model robustness by eliminating redundant predictors. The input and output features for this modeling approach are exemplified by the horizontal attitude control model, as detailed in Table 2.

Table 2
Input and output features of the horizontal attitude control model.

Input features	Attitude control features	Incremental strokes difference of gripper cylinders	Mean crown shield stroke	Mean difference of bilateral shields strokes
		Incremental stroke of thrust cylinder	Incremental crown shield stroke	Incremental difference of bilateral shields strokes
	Tunneling features	Mean thrust force	Mean clamping force of grippers	Mean cutterhead torque
		Incremental thrust force	Incremental clamping force of grippers	Mean penetration rate
	Attitude features	Required horizontal deviation adjustment	Incremental horizontal deviation	Mean horizontal deviation
	Variation features of the DTA		Advance distance	
Output features	Recommended mean strokes difference of gripper cylinders			

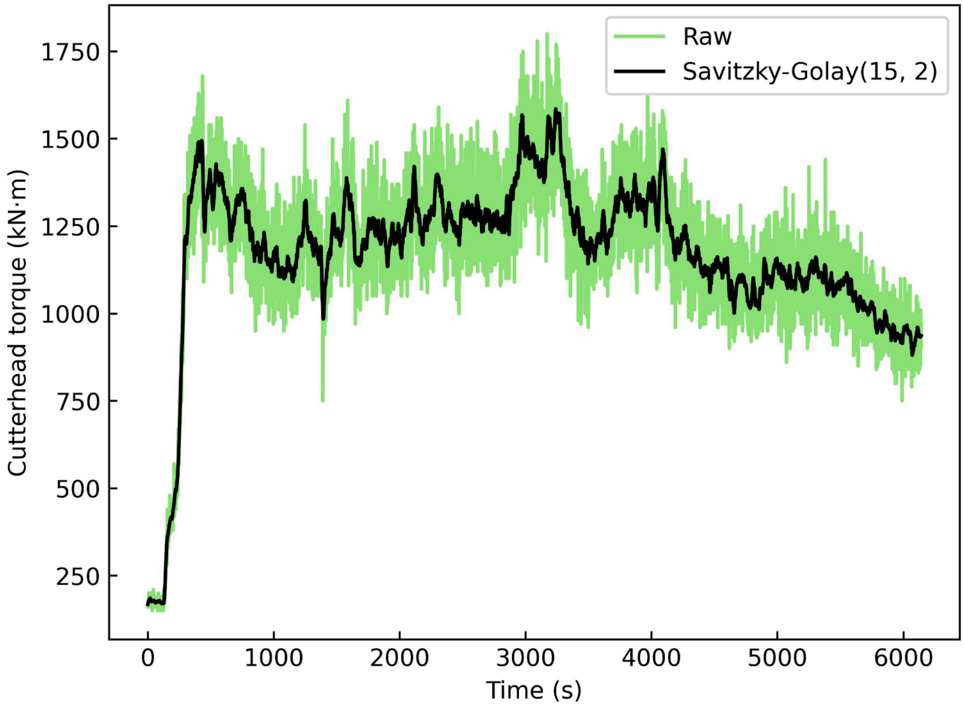

Fig. 8. Filtering of the Savitzky-Golay smoothing algorithm.

5. Establishment of database

The database integrates two primary sources: tunneling data from the onboard PLC system and guidance data from the VMT laser-guided system. The PLC system operates at dual sampling frequencies of 1 Hz and 1/60 Hz, recording 365 parameters per acquisition, such as total cutterhead thrust, torque, and penetration rate. This yields a daily volume of 86,400 or 1440 records, depending on the sampling mode. The VMT system captures the TBM's positional attitude information through laser measurements, with each entry comprising 22 distinct indices. This combined database spans the construction period from August 22, 2023 to May 25, 2024, covering a mileage of K0 + 494.700 to K4 + 043.936, which includes the third straight and curved section, and the fourth straight and curved section of the spiral ramp.

5.1. TBM tunneling cycle extraction

A single TBM tunneling cycle is defined as the complete stroke of the thrust cylinders, starting from their extension to advance the cutterhead against the excavation face. During this process, the TBM's attitude changes under the combined influence of the surrounding rock mass and internal mechanical forces. Owing to the periodic machine downtime and gripper repositioning, individual tunneling cycles must be identified and extracted from continuously recorded data. In this study, a multi-parameter combined criterion is adopted to extract effective tunneling cycles. A cycle is considered valid when the total thrust, torque, and cutterhead rotational speed all exceed zero, and the penetration rate remains below 20 mm/rev. Otherwise, the state is classified as non-tunneling. Each independent tunneling cycle corresponds to a continuous time-series segment. Due to equipment anomalies or frequent interruptions during tunneling, some cycles may be excessively short. Therefore, only those lasting longer than 600 s are retained as valid. Finally, a total of 947 valid tunneling cycles were extracted from the third straight and curved section of the spiral ramp.

5.2. Outlier detection and processing

During TBM tunneling progress, data collected by the PLC and VMT systems often contain anomalies caused by factors such as rock-excavation vibrations, heavy dust, electromagnetic interference, and operational inconsistencies. As most machine learning algorithms are sensitive to such outliers, these anomalous points must be identified and removed prior to modeling to ensure the model accuracy.

In this study, outliers are detected using the interquartile range (IQR) method, as shown in Fig. 7. The approach defines the 25th (Q1) and 75th (Q3) percentiles of the data distribution and establishes upper and lower bounds based on the IQR. Values falling outside these thresholds are considered outliers and removed from the dataset. This methodology demonstrates superior versatility compared to the conventional 3σ principle by effectively handling both normally and non-normally distributed tunneling parameters while maintaining sensitivity to extreme anomalies in each characteristic parameter of TBM tunneling data.

5.3. Data smoothing

The constructed dataset, sampled at 1/60 Hz, still contains noise due to rock–excavation vibrations, which may impair model training efficiency and prediction performance. To mitigate this, the Savitzky–Golay filter is applied to preprocess the raw tunneling data. This method employs a sliding window to perform data smoothing via local polynomial fitting, using least squares to derive adaptive weighting coefficients rather than relying on the fixed weights of the conventional mean filtering. It is observed that a longer window combined with a lower polynomial order enhances smoothing, whereas a shorter window with a higher polynomial order helps retain data details. Through parameter optimization, a window length of 15 s and a second-order polynomial were identified as the configuration that best balanced noise suppression and feature preservation. As illustrated in Fig. 8, the filtered data exhibit

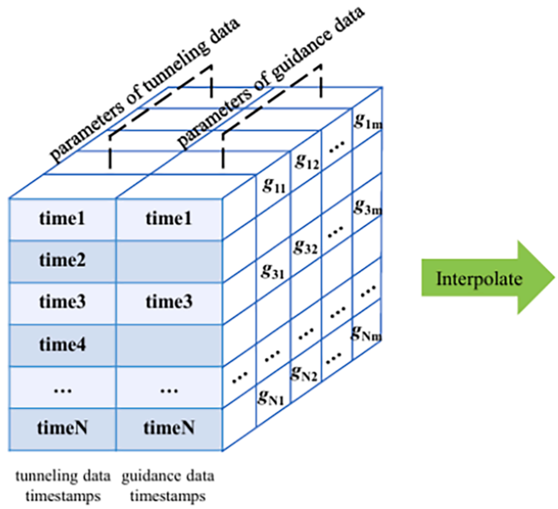

Fig. 9. Interpolation of guidance data.

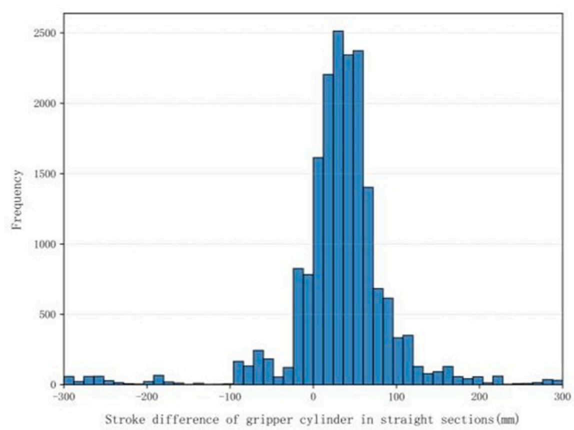

(a) Distribution in the third straight section

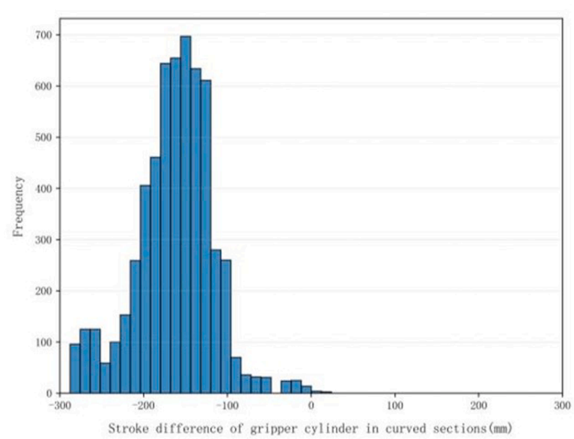

(b) Distribution in the third curved section

Fig. 10. Distribution of strokes difference of gripper cylinders.

effectively removed anomalies and significantly reduced noise, while the key data features are completely retained.

5.4. Data fusion

The fusion of guidance data and tunneling data necessitates rigorous temporal synchronization due to their distinct acquisition terminals and sampling characteristics. While tunneling data exhibit fixed-frequency recording (1 Hz or 1/60 Hz), guidance data measurements demonstrate non-uniform temporal resolution with substantially larger intervals. To ensure complete temporal correspondence between each tunneling cycle and its associated guidance data, an alignment protocol is implemented: Each tunneling cycle's start/end timestamps must be fully encapsulated within adjacent guidance data timestamps. Temporal discontinuities in guidance records are resolved through linear interpolation across missing timestamps, mathematically expressed as:

$$\widehat{V}(t) = V(t_i) + \frac{t - t_i}{t_{i+1} - t_i}[V(t_{i+1}) - V(t_i)] \tag{15}$$

Where $\widehat{V}(t)$ represents interpolated guidance parameters at missing timestamp t, bounded by adjacent measurements $V(t_i)$ and $V(t_{i+1})$. The process of constructing an integrated dataset using linear interpolation protocol was shown in Fig. 9.

This process yields an integrated dataset that not only aligns the two data domains temporally, but also establishes correlations between them. The integrated dataset, by synchronizing guidance data with tunneling parameters, captures the influence of thrust, cutterhead torque, or advance rate on the TBM's attitude deviation during specific time intervals. Such integrated dataset is particularly valuable for developing machine learning models aimed at attitude prediction and real-time control optimization. Furthermore, the integrated sequences exhibit uniform length and linear temporal distribution, meaning that each feature—whether from the guidance or tunneling system—covers consistent time spans across equal numbers of data points. This regularity significantly enhances the ability of machine learning algorithms to uncover complex coupling relationships between tunneling operations and TBM attitude changes.

The resulting methodology generates datasets featuring uniform sequence length per tunneling duration, linear temporal distribution of multi-domain features, ultimately constructing a TBM attitude database comprising 947 records. Each record corresponds to validated tunneling cycles from the third straight and curved section of the spiral ramp, with strict temporal alignment maintained through the proposed interpolation protocol.

5.5. Distribution characteristics of the control parameters

The horizontal attitude of the open-type TBM is significantly influenced by the stroke difference of the lateral gripper cylinders. Accordingly, this stroke difference is defined as the output control parameter in the horizontal attitude control model. Analysis reveals distinct distribution patterns of this stroke difference across various tunnel sections. For the "Beishan NO.1" TBM, the stroke difference of the horizontal gripper cylinders generally varies within the range of [−300, 300] mm. A statistical analysis of the stroke difference in the third straight and curved section of the spiral ramp project was conducted, with the distribution results presented in Fig. 10.

Statistical analysis of data distribution patterns reveals that under straight sections, the stroke difference of horizontal gripper cylinders is predominantly concentrated within the [−100, 100] mm range, accounting for 90.6% of cases. This distribution indicates minimal attitude adjustments during TBM tunneling in straight sections, which is consistent with the technical characteristics of linear tunneling.

Conversely, during curved sections operations, the stroke difference data demonstrates significant concentration in the [−300, 0] mm interval, comprising 99.8% of measurements. This distribution pattern reflects sustained greater extension of the right gripper cylinder compared to the left, driving the TBM into continuous right-turn tunneling mode. The distribution characteristics are strongly consistent with the alignment parameters of spiral ramp designs requiring successive right turns, while simultaneously verifying the effectiveness of gripper cylinders difference control strategies in governing TBM attitude regulation.

The horizontal attitude control of the TBM operates by varying the stroke difference between the left and right gripper cylinders, which induces a horizontal swing of the main beam and thereby alters the cutterhead orientation and tunneling direction. The range of variation v of the stroke difference is [−300, 300] mm, and the length L of the vertical line from the gripper cylinders to the cutterhead is approximately 8000 mm. Consequently, the theoretical swing angle of the cutterhead varies as follows: $\tan^{-1}\left(\frac{v/2}{L}\right) \in [-1.07^\circ, 1.07^\circ]$

5.6. Model training and evaluation

The training and test datasets were constructed using data collected from the third straight section and the third curved section of the spiral ramp, which spans from mileage K2 + 172.928 to K3 + 25.724. These data were sourced from the established attitude database. The horizontal and vertical attitude control models were developed based on their corresponding subsets of the datasets respectively. The datasets were divided into the training set and the test set according to the ratio of 80:20, with 18,792 training samples and 4698 test samples.

For both horizontal and vertical attitude control, separate models were developed in parallel. A total of 6 distinct model configurations across three different algorithm types were tested. During the training process, hyper-parameter tuning was performed using the Grid Search CV function to automatically identify the optimal combination of hyperparameters for each model.

Specifically, the hyperparameters adjusted for the LightGBM model included n_estimators, learning_rate, num_leaves, and colsample_bytree. For the XGBoost model, the tuned hyperparameters were n_estimators, learning_rate, max_depth, reg_lambda, and colsample_bytree. The

Table 3
Model hyperparameters and optimal configuration.

Models	Candidate model configuration	Best configuration	
		Horizontal model	Vertical model
LightGBM	n_estimators: [50,100,200]; learning_rate: [0.01,0.05,0.15,0.2,0.25]; num_leaves: [31,63,127,255]; colsample_bytree: [0.8,0.9,1.0]	n_estimators: 200; learning_rate: 0.2; num_leaves: 127; colsample_bytree: 0.8	n_estimators: 200; learning_rate: 0.2; num_leaves: 127; colsample_bytree: 0.8
XGBoost	n_estimators: [50,100,200]; learning_rate: [0.01,0.05,0.1,0.15,0.2,0.25]; max_depth: [3,6,9]; reg_lambda: [0, 0.1,0.5,1,2,5,10]; colsample_bytree: [0.8,0.9,1.0]	n_estimators: 200; learning_rate: 0.15; max_depth: 9; reg_lambda: 1; colsample_bytree: 0.9	n_estimators: 200; learning_rate: 0.2; max_depth: 9; reg_lambda: 1; colsample_bytree: 0.9
Random Forest	n_estimators: [50,100,200]; max_depth: [10,20,30]; max_features: [auto, sqrt]; min_samples_split: [2,5,10]; min_samples_leaf: [1,2,4]	n_estimators: 200; max_depth:30; max_features: auto; min_samples_split: 2; min_samples_leaf: 1	n_estimators: 200; max_depth:30; max_features: auto; min_samples_split: 2; min_samples_leaf: 1

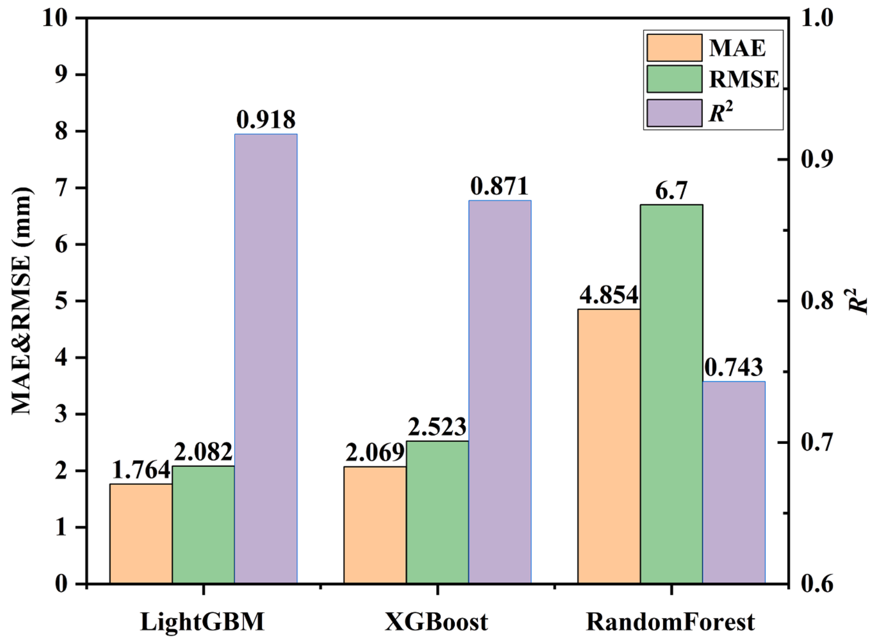

(a) Horizontal attitude control performance comparison

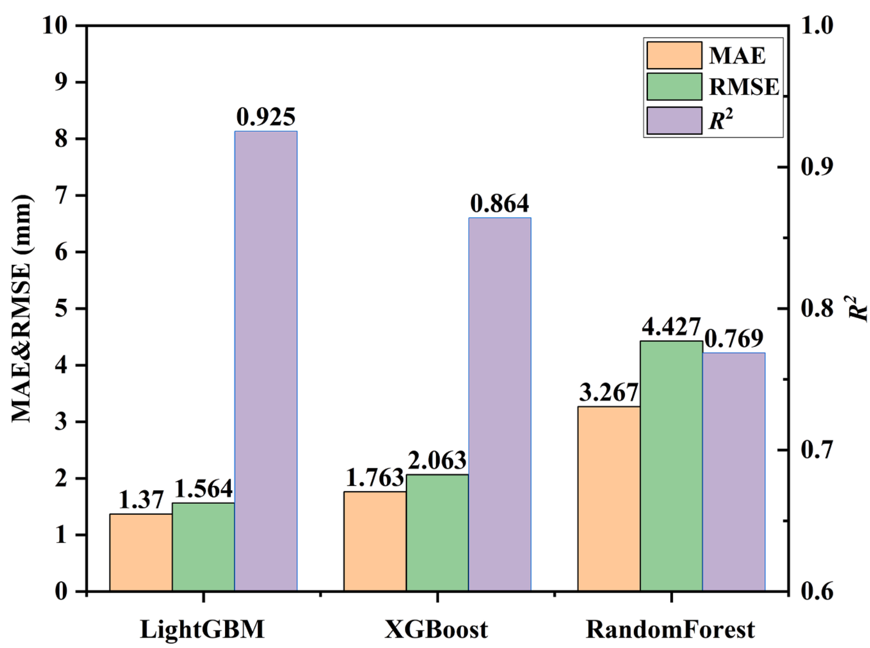

(b) Vertical attitude control performance comparison

Fig. 11. Performance comparison of horizontal and vertical attitude control models.

Random Forest model's hyperparameter optimization focused on n_estimators, max_depth, max_features, min_samples_split, and min_samples_leaf. The search ranges of the Grid Search CV function for these parameters and the final trained optimal combination identified for each model are detailed in Table 3.

Model performance was evaluated using three key metrics: Mean Absolute Error (MAE), Root Mean Square Error (RMSE), and the coefficient of determination (R^2). MAE provides a direct interpretation of the average prediction error magnitude, while RMSE, being more sensitive to larger errors, helps identify significant deviations. The ratio of MAE to RMSE offers insight into the distribution of these errors; a lower ratio suggests fewer large outliers. The R^2 score indicates the proportion of variance in the target variable explained by the model, with a value closer to 1 representing a superior fit.

$$\mathrm{MAE} = \frac{1}{m}\sum_{i=1}^{m}|(Y_i - \overline{Y}_i)| \tag{16}$$

$$\mathrm{RMSE} = \sqrt{\frac{1}{m}\sum_{i=1}^{m}(\overline{Y}_i - Y_i)^2} \tag{17}$$

$$R^2 = 1 - \frac{\sum_i (\overline{Y}_i - Y_i)^2}{\sum_i (\overline{Y} - Y_i)^2} \tag{18}$$

All model training were conducted in a Python environment utilizing PyTorch 2.1.1. The hardware platform consisted of an Intel i9–13900HX CPU and an NVIDIA GeForce RTX 4060 GPU. As previously described, the dataset was partitioned into training and testing sets with the ratio of 80:20. To ensure a robust and reliable evaluation, all six models were assessed using a 5-fold cross-validation approach. In this approach, the dataset is randomly and equally divided into five subsets. For each of the five iterations, four subsets (80% of the data) are used for training, while the remaining one subset (20% of the data) is used for testing. The final performance metrics are calculated as the average of the test results from all five iterations, providing a comprehensive evaluation of model generalization. The attitude control performance for horizontal and vertical directions was illustrated in Fig. 11.

A comparative analysis was conducted to identify the most effective model for TBM attitude control in horizontal and vertical directions. For the performance of horizontal attitude control, LightGBM achieved the most accurate predictions with an MAE of 1.764 mm, RMSE of 2.082 mm, and R^2 value of 0.918. Its RMSE/MAE ratio of 1.18 was the lowest among all three models, indicating the most stable error distribution. XGBoost exhibited moderate performance with an RMSE/MAE ratio of 1.22, while Random Forest showed the highest ratio of 1.38, suggesting relatively dispersed prediction errors.

For the vertical attitude control, LightGBM further confirmed its superiority, where it attained an MAE of 1.37 mm, RMSE of 1.564 mm, and R^2 of 0.925. And it also obtained the lowest RMSE/MAE ratio of 1.14, indicating highly stable performance for vertical prediction. These results demonstrate its strong robustness and generalization ability in modeling complex TBM behavior.

To assess the model's suitability for providing real-time instructions, its computational efficiency was evaluated on a test platform equipped with an NVIDIA RTX 3060 GPU. Across 1000 consecutive predictions with varying input data, the model achieved an average inference time of 1.600 ± 0.113 ms (mean $\pm$ standard deviation), with results ranging from 1.442 to 2.444 ms. This performance meets the requirement for real-time decision-making during TBM operation and confirms the model's feasibility for integration into an onboard TBM control system.

5.7. Feature importance analysis

This section investigates the significance of input features by evaluating their relative contributions to the predictions of the LightGBM model. As illustrated in Fig. 12, the contributions of various features to the attitude control performance in both horizontal and vertical directions are quantitatively presented.

Horizontally, the model's corrections are predominantly influenced by the *incremental strokes difference of gripper cylinders*, the *required horizontal deviation adjustment*, and *incremental horizontal deviation*, all of which attained importance scores exceeding 1895. Among these, the gripper cylinders-related feature for horizontal attitude adjustment achieved the highest importance score of 221, which aligns with the key

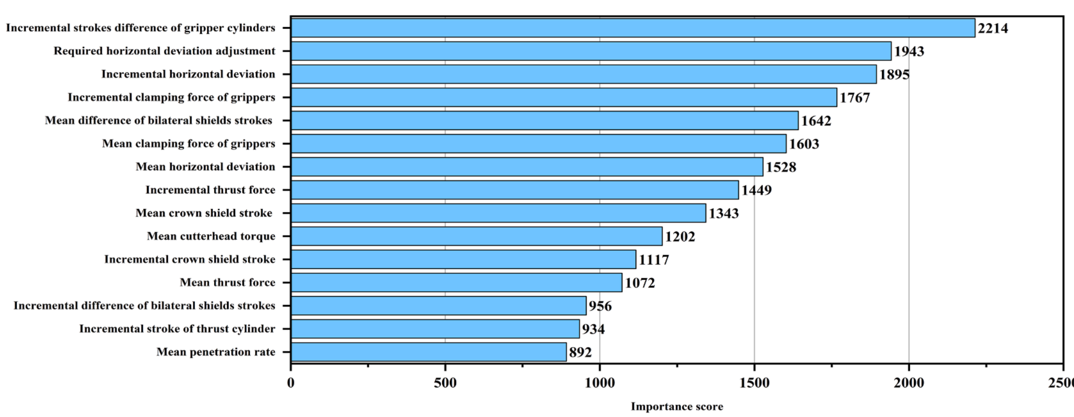

(a) Importance score for horizontal model

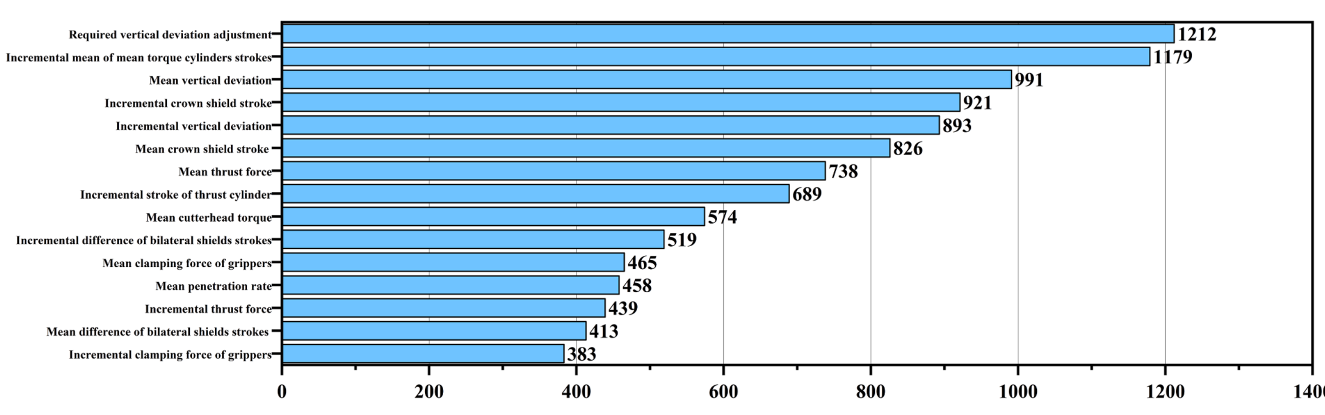

(b) Importance score for vertical model

Fig. 12. Input feature importance for attitude control models.

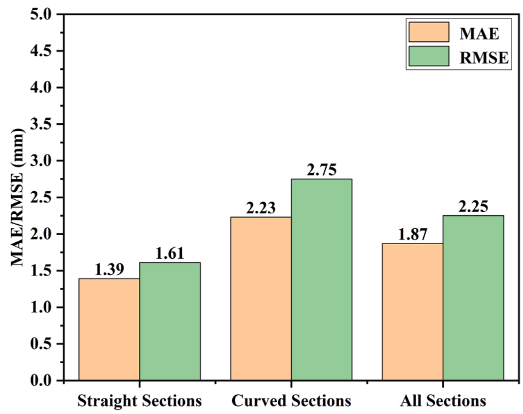

(a) Validation result: horizontal model

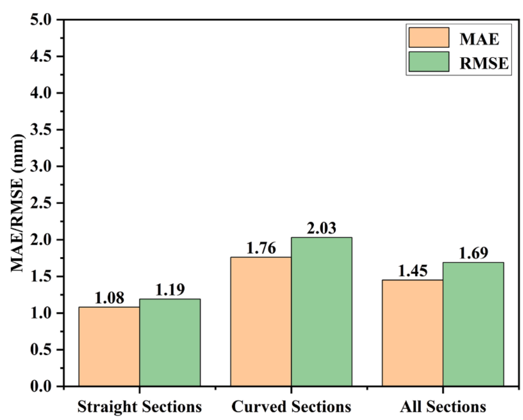

(b) Validation result: vertical model

Fig. 13. Validation results of the attitude control models.

attitude control parameter (the stroke difference between the left and right gripper cylinders) identified in the theoretical derivation (Eq. (8)). These parameters directly reflect the TBM's steering demand, making them critical inputs for effective rectification. Conversely, parameters such as the *incremental stroke of thrust cylinder* and the *mean penetration rate* showed a negligible impact, with importance scores consistently remaining below 892, suggesting they are less indicative of the TBM's steering behavior.

In the vertical direction, the model attributes high importance to the *required vertical deviation adjustment* and the *incremental mean of mean torque cylinders strokes*, both of which achieved importance scores exceeding 1179. This result aligns with the theoretical derivation (Eq. (12)), in which the mean stroke of the left and right torque cylinders is identified as the governing parameter for vertical deviation. Conversely, features such as *mean difference of bilateral shields strokes* and *incremental clamping force of grippers* demonstrated little importance, with values consistently below 413. This indicates that these variables contribute minimally to the model's generalization capability.

The close match between the data-driven feature importance ranking and the key parameters derived by theoretical equations demonstrates that the model successfully learns the underlying relationship between cylinder control parameters and cutterhead deviation. This connection enhances the interpretability of the model's predictions from an engineering perspective.

5.8. Model validation

To further evaluate the model's engineering applicability, model performance validation was conducted using field data collected from the fourth straight section and the fourth curved section of the ramp, covering the mileage interval from K3 + 25.724 to K4 + 43.936. A total of 3136 samples were included in this validation dataset. The trained models for both horizontal and vertical attitude control were validated separately under straight and curved tunneling conditions. The corresponding results are presented in Fig. 13.

The results indicate that the horizontal attitude control model achieved a MAE of 1.39 mm and RMSE of 1.61 mm in the straight section, slightly lower than the error in all sections, whereas in the curved section, it exhibited a MAE of 2.23 mm and RMSE of 2.75 mm, which are slightly higher than the performance in all sections. Similarly, the vertical control model delivered a MAE of 1.08 mm and RMSE of 1.19 mm in the straight section, and a MAE of 1.76 mm with RMSE of 2.03 mm in the curved section, also showing better performance in straight sections compared to curved sections.

The performance gap is due to the greater complexity of the curved tunneling. In straight sections, prediction error primarily causes from variable geological conditions, tunneling operational parameters, and rock-breaking vibrations. In curved sections, additional factors further contribute to the error, including the non-rigid nature of the steering mechanical structure and the continuous, coupled adjustments of multiple cylinders required for steering. These factors introduce stronger nonlinearities mapping between various features and the cutterhead deviation compared to straight sections. Although the machine learning model learns the general mapping, the increased interaction among these physical factors in curved tunneling presents a more complex relationship to capture, which leads to the performance gap between the different tunneling sections.

The validation errors remain consistent with the training and testing performance, demonstrating the model's reliability in practical applications. The proposed model is therefore capable of processing real-time tunneling and guidance data during tunneling and providing operational instructions for attitude control to TBM operators. Future work will focus on enhancing the model through enriched training data from curved sections to better capture the mapping of multiple operational parameters. Additionally, the model's practical utility will be validated through a comparative analysis of operator compliance with model recommendations versus traditional experience-based control, thereby enhance the engineering applicability of this research.

6. Conclusions

This research addresses the challenge of maintaining precise TBM attitude control along the three-dimensional spiral curve of the Beishan Underground Laboratory ramp. The theoretical steering mechanism of the open-type TBM was derived. Field data was processed through preprocessing and feature engineering to set up a comprehensive database. Through parallel comparison of three candidate machine learning models, the optimal attitude control model was identified for both horizontal and vertical control. The proposed model will be applied for practical use in guiding TBM attitude control throughout the remaining construction of the spiral ramp project. Future work will therefore focus on enhancing model generalizability across diverse geological conditions and TBM specifications, and on improving interpretability to move beyond black-box predictions toward more explicable steering guidance. The main conclusions are as follows:

(1) The steering mechanism of the "Beishan NO.1" Open-Type TBM was theoretically established, with horizontal steering mainly controlled by the stroke difference of the lateral gripper cylinders, and vertical steering mainly controlled by the mean strokes of the torque cylinders.
(2) A comprehensive TBM attitude database was established by tunneling cycle data extraction, data preprocessing, and feature

engineering. This dataset fuses tunneling features, attitude control features, attitude features, and variation features of DTA.

(3) Comparative evaluation of multiple machine learning models identified LightGBM as the top performer for both horizontal and vertical attitude control. The horizontal control model achieved an MAE of 1.764 mm and RMSE of 2.082 mm, while the vertical model achieved an MAE of 1.37 mm and RMSE of 1.564 mm.

(4) Validation conducted on both straight and curved sections of a spiral ramp showed that the horizontal control model achieved an MAE within 2.23 mm in both straight and curved sections, while the vertical control model achieved an MAE within 1.76 mm in both straight and curved sections.

CRediT authorship contribution statement

Qixin Xu: Writing – original draft, Methodology, Data curation. **Qiuming Gong:** Writing – review & editing, Project administration, Conceptualization. **Liu Huang:** Writing – review & editing. **Ju Wang:** Supervision. **Hongsu Ma:** Writing – review & editing, Supervision, Data curation. **Mengxue Qi:** Data curation. **Bei Han:** Writing – review & editing.

Declaration of Competing Interest

The authors declare that they have no known competing financial interests or personal relationships that could have appeared to influence the work reported in this paper.

Acknowledgments

This work has been supported by the China Atomic Energy Authority (CAEA) through the Geological Disposal Program.

Data availability statement

Due to the sensitive nature of the questions asked in this study, survey respondents were assured raw data would remain confidential and would not be shared.

References

[1] J. Wang, L. Chen, R. Su, et al., Beishan underground research laboratory for geological disposal of high level radioactive waste in China, World Nucl. Geosci. 40 (S1) (2023) 473–490.
[2] T. Manabe, M. Tanno, M. Matsumoto, et al., Automatic direction control technique for microtunneling machine, in: IECON'99. Conference Proceedings, San Jose, CA, USA, 1999, pp. 1295–1300.
[3] Q.C. Zhou, J.R. Chen, Z.Q. He, et al., Design of intellectualized controller of shield machine, J. Tongji Univ.(Nat. Sci.) 36 (1) (2008) 76–80 (in Chinese).
[4] G.F. Gong, K.R. Hong, T.Y. Zhou, et al., Research on shield tunneling attitude control based on fuzzy PID method, Tunn. Constr. 34 (7) (2014) 608–613 (in Chinese).
[5] H.P. Li, M.Y. Xia, Fuzzy algorithm for control of shield machine, J. Tongji Univ. (Nat. Sci.) 31 (7) (2003) 824–827 (in Chinese).
[6] Z.H. Zhang, L.H. Ma, Attitude correction system and cooperative control of tunnel boring machine, Int. J. Pattern Recognit. Artif. Intell. 32 (11) (2018) 1859018.
[7] H.Y. Yang, H. Shi, G.F. Gong, Motion control of thrust system for shield tunneling machine, J. Cent. South Univ. Technol. 17 (3) (2010) 537–543.
[8] L.T. Wang, Y. Xu, G.F. Gong, et al., Pose and trajectory control of shield tunneling machine in complicated stratum, Autom. Constr. 93 (2018) 192–199.
[9] Z.B. Liu, H.B. Xie, H.Y. Yang, Analysis and comparison of two different hydraulic thrust systems on shield tunneling machine, in: Proceedings of IEEE/ASME International Conference on Advanced Intelligent Mechatronics, Montreal, QC, Canada, 2010, pp. 563–568.
[10] H.B. Xie, X.M. Duan, H.Y. Yang, et al., Automatic trajectory tracking control of shield tunneling machine under complex stratum working condition, Tunn. Undergr. Space Technol. 32 (6) (2012) 87–97.
[11] M. Yue, Y.S. Zhang, Load observer-based integral sliding mode trajectory tracking control of shield automatic tunnelling via hyperbolic tangent function, Int. J. Model. Identif. Control 25 (2) (2016) 111–118.
[12] M. Hu, B.J. Wu, X.W. Gao, et al., Real-time deviation correction system and method for shield tunneling based on big data, Chinese Patent CN109779649A, 2019. (in Chinese).
[13] S.L. Zhu, L.H. Lu, J.C. Sun, et al., Shield machine positioning and deviation correction system integrating stratum information, Chinese Patent CN105736007A, 2016. (in Chinese).
[14] Z. Zhang, G.F. Gong, W.Q. Wu, et al., Adaptive attitude control of thrust system for hard rock tunnel boring machine, J. Zhejiang Univ.(Eng. Sci.) 49 (10) (2015) 1870–1877 (in Chinese).
[15] H.B. Zhang, J. Ji, G. Wang, Application of grey predictor algorithm on the synchronous control of TBM propulsion system, J. Mach. Des. 35 (2) (2018) 1–5 (in Chinese).
[16] Z. Peng, G.F. Gong, H.Y. Yang, et al., The vertical adjustment system with angle closed loop control for TBM, in: 12th IEEE/ASME International Conference on Mechatronic and Embedded Systems and Applications (MESA), Auckland, New Zealand, 2016, pp.1–6.
[17] H.J. Liu, J.C. Wang, L.W. Zhang, et al., Dynamic modeling and trajectory tracking control of tunnel boring machine, in: The 26th Chinese Control and Decision Conference, Changsha, China, 2014, pp. 4560–4565.
[18] M.J. Zhang, Research on auto rectification and posture control of the boom-type roadheader, PhD Thesis, China University of Mining and Technology (Beijing), 2019. (in Chinese).
[19] T. Liu, Study on the attitude adjusting and cutterhead driving system of hard rock tunnel boring machine, PhD Thesis, Zhejiang University, 2025. (in Chinese).
[20] C.J. Shao, J.F. Liao, Z.T. Liu, et al., Indirect adaptive robust trajectory tracking control of hard rock TBM with load variation of tunneling face, Chin. J. Mech. Eng. 32 (2019) 34.
[21] C.J. Shao, J.F. Liao, Z.T. Liu, et al., Trajectory tracking control in horizontal direction of open-type hard rock tunnel boring machine based on adaptive robust control strategy, J. Mech. Eng. 54 (1) (2018) 113–119.
[22] J. Wang, L. Chen, R. Su, et al., The Beishan underground research laboratory for geological disposal of high-level radioactive waste in China: Planning, site selection, site characterization and in situ tests, J. Rock Mech. Geotech. Eng. 10 (3) (2018) 411–435.
[23] H.S. Ma, J. Wang, K. Man, et al., Excavation of underground research laboratory ramp in granite using tunnel boring machine: Feasibility study, J. Rock Mech. Geotech. Eng. 12 (6) (2020) 1201–1213.
[24] J. Wang, M.X. Qi, B. Long, et al., Technical innovation in the “Beishan No.1” hard rock tunnel boring machine for high-gradient spiral tunnels, Front. Eng. Manag. 11 (1) (2024) 175–179.
[25] N.B. Li, Intelligent decision-making method for TBM tunneling parameters and attitude based on rock mass geological information perception, PhD Thesis, Shandong University, Jinan, 2022. (in Chinese).
[26] X.X. Zhou, Q.M. Gong, L.J. Yin, et al., Predicting boring parameters of TBM stable stage based on BLSTM networks combined with attention mechanism, Chin. J. Rock Mech. Eng. 39 (S2) (2020) 3505–3515.

Prof. Qiuming Gong received his Ph.D. degree from Nanyang Technological University (NTU), Singapore, in 2006, a Master’s degree from the Institute of Geology, Chinese Academy of Sciences (CAS), in 1995, and a Bachelor’s degree from Xi’an College of Geology (now part of Chang’an University) in 1992. From 1995–2001, he worked at the Beijing Institute of Geo-Engineering Exploration & Surveying (BIGE). Between 2005 and 2006, he served as a Project Officer at the Protection Engineering Research Centre (PERC), NTU, conducting research on tunnel excavation. Since late 2006, he has been affiliated with the College of Architecture and Civil Engineering, Beijing University of Technology, where he holds the positions of Associate Researcher and later Professor. In 2006 and 2011, he was invited as a Visiting Scientist and later as a Visiting Professor to the Laboratoire de Mécanique des Roches (LMR) at the Swiss Federal Institute of Technology Lausanne (EPFL). Prof. Gong specializes in geotechnical and tunnel engineering. He serves as an Editorial Board Member for the international journal *Tunneling and Underground Space Technology* and holds council memberships in several committees of the Chinese Society for Rock Mechanics and Engineering (CSRME). He authored and co-authored four monographs and holds more than 50 national invention and utility model patents. He has published over 100 academic papers, including more than 50 international journals, and his work has garnered over 3000 SCI citations.